METALLIC NANOTOXICITY TO BACTERIA AND BACTERIOPHAGE

A Thesis

presented to

the Faculty of the Graduate School

at the University of Missouri

In Partial Fulfillment

of the Requirements for the Degree

Master of Science

by

JIA YOU

Dr. Zhiqiang Hu, Thesis Supervisor

MAY 2010

The undersigned, appointed by the Dean of the Graduate School, have examined the thesis entitled

METALLIC NANOTOXICITY TO BACTERIA AND BACTERIOPHAGES

Presented by Jia You,

A candidate for the degree of Master of Science,

And hereby certify that, in their opinion, it is worthy of acceptance.

_____

Dr. Zhiqiang Hu

_____

Dr. Enos C. Inniss

_____

Dr. Matthew Bernards

ACKNOWLEDGEMENTS

I would like to express my sincere thanks to my advisor Dr. Zhiqiang Hu, in the Department of Civil and Environmental Engineering, for his precious and tireless advice, encouragement and support all throughout my graduate studies.

I also want to extend my thanks Dr. Enos Inniss in the Department of Civil and Environmental Engineering and Dr. Matthew Bernards in the Department of Chemical Engineering for being my graduation thesis committee. Their guidance and enthusiasm is greatly appreciated.

Besides, I am grateful to postdoctoral fellow, Dr. Jianzhong Zheng and graduate students, Zhihua Liang, Atreyee Das, Shashikanth Gajaraj, Yu Yang, Qian Chen, Yanyan Zhang, Jia Guo, Hilda F. Khoei, Meng Xu and Shengnan Xu, whose cooperation and help means a lot to me.

Last but not least, I would like to convey a special thanks to my beloved parents, whose moral encouragement and support helped me realize my master's degree goal.

TABLE OF CONTENTS

LIST OF TABLES

LIST OF FIGURES

Figure Page

ABSTRACT

The inhibitory effort of two commonly used nanoparticles, silver nanoparticles (Ag NPs) and zinc oxide nanoparticles (ZnO NPs), on the growth of bacteria (*E. coli*) and bacteriophage (MS2) were evaluated using a turbidimetric microtiter assay and the standard double agar layer (DAL) assay. In the pure *E. coli* cultures, Ag NPs presented a greater degree of inhibition against bacteria than ZnO NPs. However, both nanoparticles did not deactivate MS2 at the highest nanoparticle concentrations tested (5 mg/L total Ag and 20 mg/L ZnO). Instead, exposure of MS2 to ZnO NPs at the concentration of 20 mg/L ZnO resulted in significantly higher plaque forming units (PFU) than the control. No bacteriophage inactivation was observed in the presence of nanosilver, nanosilver/Ag^+ mixture (50:50 of Ag^+ and nanosilver in mass ratios) or Ag^+ ions, all at the total Ag concentration of 5 mg/L. In a binary system containing bacteria and phages, both MS2 and Ag NPs reduced bacterial growth, but the degree of bacterial growth inhibition by nanosilver or a mixture of nanosilver/Ag^+ was phage concentration dependent. For Ag^+ ions at concentration of 5 mg/L Ag, complete bacterial growth inhibition was observed regardless of phage concentration. Results from the dynamic bacterial growth inferred from the turbidimetric microtiter assay and the parallel active bacterial and phage concentration measurements inferred from standard agar plate assay indicated that both Ag NPs and ZnO NPs facilitated MS2 to infect the *E. coli* host. The complex interactions among bacteria, phage and nanoparticles suggested that bacterial cell

membrane disruption or structure change due to nanoparticle exposure might allow bacteriophage MS2 to enter bacterial host cells more easily and promote bacterial cell lysis.

CHAPTER 1 INTRODUCTION

1.1 Nanoparticles and Nanotechnology

Nanoparticles are commonly defined as particles with the size of at least one dimension ranging from 1 to 100 nm ("National Nanotechnology Initiative" http://www.nano.gov/), which serve as a bridge between bulk materials and atoms/molecules (Nel et al. 2006). In recent decades, nanoparticles have been applied in many areas because of their unique size-dependent physicochemical, electromagnetic, optical, and chemical catalytic properties (Table 1) (Gun'ko et al. 2009; Sreeja et al. 2009; Zhang et al. 2009; Khlebtsov et al. 2010).

Nanotechnology is referred to as the emerging technology involving fabrication or application of nanosized structures or materials (Maynard et al. 2006). Of the three main exploration levels (materials, devices and systems), nanomaterials show trends in continuous and the most advanced development (Maynard et al. 2006). Nanomaterials display enhanced or unique properties due to their large surface to volume ratio and specific crystallographic surface structure compared to bulk materials (Ruben et al. 2005) which bring their applications in various industries (Table 2). Many of these nanomaterials are often stored in powder form. However, they might aggregate rapidly, especially when they are resuspended in water. Particle

aggregation may greatly affect the property of the nanomaterials and their potential applications.

Table 1. Properties and current applications of nanoparticles

Property	Applications
Optical	Anti-reflection coatings
	Tailored refractive index of surfaces
	Light based sensor for cancer diagnosis
Magnetic	Improved details and contrast property in MRI images
	Increased density storage media
Thermal	Enhance heat transfer from solar collectors to storage tanks
	Improved efficiency of coolants in transformers
Mechanical	Improved wear resistance
	New anti-corrosion properties
	New structural materials, composites, stronger and lighter
Electronic	High performance and smaller components, e,g, capacitors for small consumer devices such as mobile phones
	Displays which are cheaper, larger, brighter, and more efficient
	High conductivity materials

Table 2. Specific applications of nanomaterials

Area	Applications
Energy	High energy density and more durable batteries
	Hydrogen storage applications using metal nanoclusters
	Electro catalysts for high efficiency fuel cells
	Renewable energy, ultra high performance solar cells
	Catalysts for combustion engines to improve efficiency
Biomedical	Antibacterial silver coatings on wound dressings
	Sensors for disease detection (quantum dots)
	Programmed release drug delivery systems
Environmental	Clean up of soil contamination and pollution
	Biodegradable polymers
	Aids for germination
	Treatment of industrial emissions
	More efficient and effective water filtration
Others	Activity of catalysts
	Coatings for self cleaning surfaces
	Effective clear inorganic sunscreens

1.2 Antibacterial Behaviors of Ag and ZnO Nanoparticles

Of all the promising nanomaterials, metallic nanoparticles such as silver nanoparticles (nanosilver or Ag NPs) have been drawing great attention due to their unique antibacterial properties and low toxicity to mammalian cells (Ruben et al. 2005; Maynard et al. 2006; Mühling et al. 2009). They have been used in various areas, including cosmetics, paints, food storage containers and clothing (Barry et al. 2004; Ruben et al. 2005; Morones et al. 2005; Lok et al. 2006; Lok et al. 2007; Pal et al. 2007; Choi et al. 2008). The antimicrobial characteristics of Ag NPs can be traced back to the use of silver products in human history. For instance, ancient Greek cooked in silver pots and silver materials were used as biocides in treating burns and wound dressings (Klasen 2000).

In general, Ag NPs can be obtained from commercial sources (Ruben et al. 2005) or newly synthesized in the lab. One common nanosilver fabrication method is the reduction of Ag^+ ions ($AgNO_3$) using borohydride ($NaBH_4$) as a reducing agent in the presence of stabilizing agents such as sodium citrate or PVA (Polyvinyl Alcohol) solution (Lok et al. 2006; Lok et al. 2007; Choi et al. 2008). Different distribution of Ag NPs can be obtained by adjusting the molar ratio of BH_4^-/Ag^+ (Choi et al. 2008). Ag NPs can also be made through biosysthesis-based method (Birla et al. 2009).

The antibacterial behaviors of Ag NPs are generally shape, size, and concentration dependent (Yamamoto 2001; Sondi et al. 2004; Adams et al. 2006; Lok et al. 2006; Pal et al. 2007; Zhang et al. 2007; Choi et al. 2008; Choi et al. 2008; Jones et al. 2008). It was reported that ZnO NPs with a truncated triangular shape had the strongest biocidal action on *Escherichia coli* (*E. coli*) followed by spherical and rod shape, based on test concentrations of 10, 125 and 1000 mg/L (Pal et al. 2007). *E. coli* is one commonly used Gram-negative rod-shape bacterial strains for antibacterial test. Recent studies showed that 10 mg/L Ag NPs (average particle size = 12 nm) reduced *E. coli* growth by 70% (Sondi et al. 2004) while Ag NPs (average particle size = 14 nm) caused 55% growth inhibition on *E. coli* PHL628-gfp at a much lower concentration (0.45 mg/L) (Choi et al. 2008). Another study also demonstrated that the MIC (minimum inhibitory concentration, determined while no visual turbidity was observed) and MKC (minimum killing concentration, determined by the lack of visual turbidity after reinoculation) of Ag NPs (particles size ranging from 2 ~ 5 nm) against *E. coli* were 22.6 and 28.3 mg/L, respectively (Gogoi et al. 2006).

In addition to the properties of Ag NPs, initial bacterial concentration also serves as another important factor in determining antibacterial action. Previous studies showed that when treated with the same concentration of Ag NPs of 20 mg/L Ag (average particle size = 12 nm), only a delay of bacterial growth occurred at the initial *E. coli* concentration of 10^7 CFU/mL, while a decrease of bacterial colony number was

observed at the initial *E. coli* concentration of 10^5 CFU/mL. A complete inhibition of *E. coli* growth was observed when the initial *E. coli* concentration reduced to 10^4 CFU/mL (Sondi et al. 2004).

Although the antibacterial behavior of Ag NPs is generally concentration dependent, studies also revealed that an increased concentration of Ag NPs above 2 mg/L does not increase nano-toxicity against the naturally occurring bacteria in estuarine sediment samples, which was assumed to be related to the bioavailability of the nanoparticles under the conditions of high salt concentrations (Mühling et al. 2009). Similarly, high electrolyte content in the media might also lead to the loss of antibacterial effects of Ag NPs on *E. coli* (Lok et al. 2007).

Similar to Ag NPs, Zinc oxide nanoparticles (ZnO NPs) also raise great interest due to their various applications in photocatalytic, antibacterial, electronic, optical, electrical, dermatological and medical areas (Turkoglu et al. 1997; Pan et al. 2001; Sawai 2003; Xiong et al. 2003; Behnajady et al. 2006; Tang et al. 2006). Besides, ZnO NPs are also widely applied to products such as sunscreens and special textiles due to their predominant ultraviolet (UVA and UVB) blocking properties and low toxicity to human beings (Becheri et al. 2008; Newman et al. 2009).

Analogue to Ag NPs, the antibacterial behavior of ZnO NPs is also size, concentration and shape dependent, with relatively lower toxicity as compared to Ag NPs. Zn NPs with mean size around 20 nm and 480 nm are reported to inactivate *E. coli* at concentration of 20 and 1000 mg/L, respectively (Adams et al. 2006; Zhang et al. 2007; Jiang et al. 2009). Studies showed that viable colony counts of *E. coli* and *B. atrophaeus* decreased as the concentration of ZnO NPs increased, with no viable colonies observed at ZnO NPs concentrations of 1500 and 200 mg/L ZnO, respectively (Tam et al. 2008). An enumeration assay via standard agar plates also revealed that ZnO NPs caused about 95% inhibition of *S. aureus* and *S. agalactiae* proliferation at a concentration of 8000 mg/L ZnO, while only 30% inhibition of bacterial growth was observed at the ZnO NPs concentration of 800 mg/L ZnO (Huang et al. 2008). ZnO NPs may cause different degrees of inhibition to different microbial strains. For instance, ZnO NPs inhibited *B. subtilis* (G-positive bacteria) growth by 90% at a concentration of 10 mg/L ZnO, while only reducing *E. coli* growth by 48% at a concentration of 1000 mg/L ZnO (Adams et al. 2006). Furthermore, the antibacterial action of ZnO NPs is caused by some external factors, such as light intensity, particle morphology, and chemical modification/composition (Adams et al. 2006; Hui Yang 2009).

1.3 Possible Mechanisms of Antibacterial Action by Ag NPs

Recent studies have demonstrated that the antibacterial action of Ag NPs may be assumed due to both nano-Ag and Ag^+ ions, which are released from nano-Ag suspension (Sondi et al. 2004; Ruben et al. 2005; Choi et al. 2008).

Part I: Toxicity due to Ag^+ ions

As reported by relevant studies, Ag^+ ions may be gradually released from naonosilver particles, which are coupled with silver oxidation (Equation 1).

$$4Ag + O_2 + 2H_2O = 4Ag^+ + 4OH^- \quad \text{(Equation 1)}$$

Since silver has a tendency to interact with sulfur- or phosphorus-containing soft bases (e.g. R-S-R, R-SH or RS^-), it is highly possible that some functional groups which contain sulfur-containing proteins (e.g. enzymes on the membrane) and phosphorus-containing elements (e.g. DNA) will binding with Ag^+ ions, which cause malfunction of those molecular groups (Sondi et al. 2004; Kumar et al. 2005; Yamanaka et al. 2005; Mühling et al. 2009). After Ag^+ ions treatment, bacterial DNA loses its capability to replicate, to express ribosomal subunit proteins became inactivated, and some cellular proteins and enzymes which are essential for ATP production (Yamanaka et al. 2005). Ag^+ ions was also hypothesized to affect the membrane-bound enzymes function (e.g. enzymes involved in the respiratory chain) and facilitate the generation of ROS (McDonnell et al. 1999; Pal et al. 2007). In

addition, the electrostatic force between Ag^+ ions and the negatively charged cell membrane/wall may result in the inhibition of respiratory chain enzyme, the change of membrane permeability and ultimate cell lysis and death (Ratte 1999; Sambhy et al. 2006). Although research has revealed that some bacteria might have self-defense mechanisms or silver resistant properties (Silver 2003; Morones et al. 2005), Ag NPs are generally viewed as an excellent antimicrobial agent.

Part II: Toxicity contributed by nanosilver

The possible mechanisms of inhibitory affects of Ag NPs against bacteria were speculated to be similar to Ag^+, although studies show no direct interactions occurred between Ag NPs and cell DNA or protein profiles (Gogoi et al. 2006). Overall, nanosilver toxicity is size, shape, and concentration dependent. The degree of inhibition also depends on the initial microbial concentration (Pal et al. 2007).

The antibacterial mechanisms of Ag NPs are related to the interaction between nanoparticles and bacterial cells, resulting in membrane property changes, followed by increased membrane permeability and dysfunction of molecular transportation through the plasma membrane (Sondi et al. 2004; Ruben et al. 2005; Lok et al. 2006). The attachment of Ag NPs to cell membrane surfaces and possible penetration of Ag NPs inside the bacterial cells may affect electron transfer in the respiratory chain,

proton motive force and ATP pool, which might be related to the high affinity of silver to some phosphorus-containing protein (located on membrane surface) and sulfur-containing materials mainly located inside the cell (Ruben et al. 2005; Choi et al. 2008).The attachment of Ag NPs to the vicinity of the bacterial cell wall might reduce its oscillator strength, leading to the decrease of fluorescence intensity from the cell (Sondi et al. 2004; Gogoi et al. 2006).

Recently research also demonstrated that Ag NPs might cause bacterial cell structure change through the formation of "pits" on the surface (Amro et al. 2000), consistent with similar findings that Ag NPs could attach to nitrifying bacterial cells, resulting in cell wall pitting (Choi et al. 2008). The change of cell morphology resulted in a notable increase in cell permeability by the release of lipopolysaccharide (LPS) molecules and membrane proteins, although the outer cell membrane is mainly constructed by the tightly packed LPS molecules (Raetz 1990). As a result, the bacterial cell loses the capability of proper transport regulation via the cell membrane (Amro et al. 2000; Amro et al. 2000; Sondi et al. 2004). Ag NPs cause the loss of replication ability of DNA and inactivation of cellular proteins (Feng et al. 2000; Lok et al. 2006), eventually leading to the cell death.

The oxidation of Ag NPs often leads to the formation of partially oxidized Ag NPs with chemisorbed Ag^{+} (Henglein 1998; Henglein 2002). Studies have shown that the

partial oxidation of Ag NPs, which correlates with the change of the surface plasmon resonance adsorption present higher toxicity (Lok et al. 2007). In addition to oxidation, the crystallization, aggregation and dissolution involved in the bacteria-NPs interactions are responsible for the antibacterial action of Ag NPs (Sondi et al. 2004; Choi et al. 2008).

While few studies indicate a the direct effect of Ag NPs on protein expression or intracellular DNA replication, it is suggested that the generation of intracellular reactive oxygen species (ROS) due to Ag NPs or Ag^{+} ion exposure might damage cellular constituent and disrupt cell function, which provides an additional toxicity mechanism (Gogoi et al. 2006; Kim et al. 2007; Choi et al. 2008).

1.4 Possible Mechanisms of Antibacterial Action by ZnO NPs

Several mechanisms for the antimicrobial action by ZnO NPs have been proposed. These include the disruption of cell wall and membrane integrity, generation of reactive oxygen species and free radicals (Adams et al. 2006; Zhang et al. 2007).

First of all, electron micrographs have shown that ZnO nanoparticles damage the bacterial cell wall, increase cell membrane permeability, and change the cell morphology (Adams et al. 2006; Zhang et al. 2007; Huang et al. 2008), which was

assumed to be due to the interactions of ZnO NPs with bacterial membrane surface (e.g. the cellular internalization of ZnO NPs). This resulted in the membrane dysfunction (Nair et al. 2008), change of membrane permeability, leakage of intracellular substrates (Zhang et al. 2007; Huang et al. 2008) and finally cell death. Nair *et al*. attributed this interaction to electrostatic effects due to the opposite surface charges of nanoparticles and cell membrane (Nair et al. 2008). These speculations were supported by the fact that starch-capped ZnO NPs are less toxic due to the protection caused by the OH-related quenching of the nanoparticle positive charge (Nair et al. 2008).

The proposed mechanism could also explain why Gram-positive bacteria (e.g. *S. aureus*) were less sensitive to the nanoparticles than the Gram-negative bacteria (e.g. *E. coli*). Because Gram-positive bacteria have a thicker peptidoglycan cell wall than G-negative bacteria, it is likely more difficult for ZnO NPs to induce membrane damage (Nair et al. 2008).

Furthermore, the increase of oxidative stress as generated by ZnO NPs may also lead to the observed cyto-toxicity, followed by the cell death and the significant change of crystal structure of ZnO NPs (Huang et al. 2008).

ZnO NPs may release Zn^{2+} like Ag NPs which can slowly and continuously release Ag^{+} (Choi et al. 2008). Although Roselli et al. demonstrated that Zn^{2+} could be

metabolized by *E. coli* as an oligoelement (Roselli et al. 2003), which functioned as cofactors, coenzymes, catalysts and so on (Gaballa et al. 1998), excess Zn^{2+} is toxic to the bacteria, causing the dysfunctions of important Zn-containing proteins and enzymes (Xiong et al. 1998).

The concentrations of ZnO NPs used in our experiments were relatively low (10 and 20 mg/L). ZnO NPs may therefore cause negligible inhibitory effects on *E. coli* growth. On the contrary, ZnO NPs might release Zn^{2+} that facilitates the growth of *E. coli*.

Another well accepted mechanism for the inhibitory effects of nanosized metal oxide particles (e.g. ZnO, TiO_2 and SiO_2) on bacteria (e.g. *E. coli* and *B. subtilis*) is the generation of reactive oxygen species (ROS) in the presence of light (Adams et al. 2006). Unlike Ag NPs, the generation of photocatalytic ROS in the presence of UV or sunlight serve as an important factor for the antibacterial action of ZnO NPs (Adams et al. 2006; Jones et al. 2008). It is noted that the production of ROS such as hydrogen peroxide (H_2O_2) could damage cell membranes, causing dysfunction of cellular components, and leading to final cell death (Tam et al. 2008). Light (or UV exposure) is the essential factor for generating the photocatalytic properties of those metallic oxide nanoparticles, although the inhibitory results observed under dark conditions implied the existence of some other unknown mechanisms.

In a binary system containing bacteria and bacteriophage, it is speculated that the formation of "pits" on the bacterial cell wall and membrane permeability increase as a result of nanoparticle exposure may help the virus enter or leave the cell more easily. The changes of bacterial cell structure and increasing membrane permeability help cell lysis by bacteriophage, as demonstrated using the standard double agar layer assay and turbidimetric microtiter assay. By monitoring the dynamic bacterial growth through the microtiter method, more insightful information on bacterium-virus interactions can be obtained and possibly used for mathematical modeling of the dynamics of viral infections (Campos et al. 2008).

1.5 The Antiviral Action of Ag and ZnO NPs and Possible Mechanisms

While a wealth of research has demonstrated the antibacterial potential of Ag and ZnO NPs against bacteria, little is known about the antiviral effect of these nanoparticles. Enteric viruses are present in both natural and engineered (water and wastewater) environments (Nasser et al. 1995). Due to a similar morphology to hepatitis A virus and polioviruses, MS2 (F-specific single-stranded RNA bacteriophage, with diameters of 24-26 nm) is widely used as a surrogate for enteric viruses (Havelaar et al. 1993). Inactivation of viruses is of great importance to both the natural and engineered environments. Several effective methods have been widely applied to remove and inactivate viral activities. These include coagulation, ultraviolet radiation, and disinfectant by free chlorine, chlorine dioxide, and ozonation (Sobsey et

al. 1998; Shin et al. 2003; Thurston-Enriquez et al. 2003; Shirasaki et al. 2009). Currently, inactivation of viruses by nanoparticles is an emerging area of research and development with the potential for developing more efficient antiviral agents.

A recent study showed that Ag NPs (particle size range from 1 to 10 nm) coated with foamy carbon, poly (N-vinyl-2-pyrrolidone) (PVP), or bovine serum albumin (BSA) almost completely killed HIV-1 viruses after 24 h treatment at concentrations higher than 10 mg/L (Elechiguerra et al. 2005). At concentrations above 12.5 mg/L, polysaccharide coated Ag NPs (particle size around 10 nm) significantly decreased the observed mean plaque forming unit of monkey pox virus (MPV) (Rogers et al. 2008). Ag NPs (particle sizes: 10 and 50 nm) also stopped hepatitis B virus replication by inhibiting RNA production (Lu et al. 2008). These results indicate the potential of using Ag NPs at relatively high concentrations (e.g., above 10 mg/L Ag) to provide cyto-protective activities towards virus-infected mammal cells.

The mechanisms involved in the antiviral behaviors of nanoparticles are still not well elucidated. It is suggested that Ag NPs (size range from 1 to 10 nm) may restrain the HIV-1 from binding to the host cell by interacting with the gp 120 glycoprotein knobs of the virus (Elechiguerra et al. 2005). Another antiviral study using Ag NPs and monkeypox virus (MPV) proposed two mechanisms including blockage of binding to host cell by physical obstruction and disruption of host cell biochemical pathway,

both of which affect viral replication (Rogers et al. 2008). Studies also show that the presence of ROS (reactive oxygen species) via UV photosensitization of fullerol nanoparticles contributes to viral MS2 inactivation. The 1st-order inactivation rate doubled in the presence of singlet oxygen and increased by 125% in the presence of both singlet oxygen and superoxide (Badireddy et al. 2007), which are all related to fullerol photosensitization.

1.6 Research Objectives

Since a wide variety of microorganisms including bacteria, virus, and protozoa are present in the engineered system (e.g., wastewater treatment plants) and the natural environment, it is important and necessary to study and compare the inactivation properties of nanoparticles against bacteria and bacteriophage, both of which are of significance to public health and the environment. However, since the concentrations of nanoparticles such as Ag NPs in the engineered system or the natural environment are unlikely to reach the high levels as described earlier, relatively low concentrations of Ag NPs (< 5 mg/L) and ZnO NPs (< 20 mg/L) were evaluated in this study. The main objective of this study was to evaluate the inhibitory effect of Ag and ZnO NPs on the growth of *E. coli* and bacteriophage MS2 in a binary system (bacteria-phages) using a turbidimetric microtiter assay and the standard double agar layer method.

CHAPTER 2 MATERIALS AND METHODS

2.1 Nanoparticle Preparation and Characterization

Silver nanoparticles. Silver nanoparticles were made from 0.7 mM $AgNO_3$ (EM Science) by adding sodium borohydride ($NaBH_4$, Sigma) with polyvinyl alcohol (PVA) as a capping agent. Sodium borohydride was added into a 0.06% (wt) PVA solution, and silver nitrate was then rapidly injected at room temperature. The freshly prepared nanoparticle suspensions (0.7 mM or 76 mg/L) included roughly 50:50 of Ag NPs and Ag^+ ions in mass ratio (hereafter referred to as 50% AgNPs) and almost complete Ag nanoparticle in the form of Ag NPs (hereafter referred to as 100% AgNPs) by adding $NaBH_4$ at the concentrations of 0.14 and 0.7 mM, respectively. To reduce the likely adverse effects brought by particle dissolution and agglomeration, nanosilver suspensions were freshly made before each experiment and characterization.

Zinc Oxide Nanoparticles. The ZnO NPs with 99.6% purity was purchased in commercial powder form (advertised particle size = 20 nm, Nanostructured & Amorphous Materials Inc., NM). ZnO NPs stock (200 mg/L) was prepared by adding 100 mg zinc oxide powder to 500 mL de-ionized water, coupled with continuous stirring at 700 rpm. To help the homogeneous suspension of ZnO NPs, sonication (for

up to 20 min, Model 100 Sonic Dismembrator, Fisher Scientific) was employed every time before use.

Nanoparticle Characterization. Transmission electron microscopy (TEM, JEOL 1400) was applied to determine the particle size distribution of the Ag NP and ZnO NP suspension and their average particle size. An aliquot of Ag and ZnO nanoparticle suspension (1 µl) was added onto a standard copper-coated TEM grid and images were recorded under an accelerating voltage up to 100 keV. The real particle size distribution generated from TEM images were analyzed by using ImageJ, a Java-based image processing software available at http://rsb.info.nih.gov/ij/.

2.2 Bacteria Cultivation and Bacteriophage MS2 Propagation.

Bacterial Culture. *E. coli* (ATCC 15597) was selected as a model organism not only because it is a commonly studied K-12 strain with known genomic information (Blattner et al. 1997), but also it is a recommended host cell strain of bacteriophage MS2. The strain was freshly cultivated in a Luria-Bertani (LB, ACROS, New Jersey) medium at 37 ^{o}C on a shaker at 150 rpm overnight each time before use. The bacterial stocks (typical concentration =10^{8} CFU/mL, enumerated by the standard plate assay) were used in subsequent experiments with required working dilutions in

1× phosphate buffer saline (PBS, containing 137 mM NaCl, 2.7 mM KCl, 1.4 mM Na_2HPO_4 and 4.3 mM $Na_2HPO_4 \cdot 1H_2O$, pH 7.2).

Bacteriophage MS2 Propagation. *E. coli* bacteriophage MS2 (ATCC 15597-B1), a single-stranded RNA coliphage, was selected as a model virus in this study. Bacteriophage stocks were propagated using the double agar layer (DAL) method (Adams 1959; Badireddy et al. 2007). Approximately 100 μL of bacteriophage, 200 μL of host bacteria (*E. coli* ATCC 15597 culture freshly cultivated overnight), and 5 mL LB containing 0.5% molten agar (with 0.1% glucose, 2 mM $CaCl_2$ and 0.1 mg/mL Thiamine) agar were poured onto plates containing 1.5% agar. The plates were incubated at 37 ℃ overnight. Bacteriophage stocks were collected the following day by adding 10 mL of 1× PBS to the surface of the plate and allowing it to incubate at room temperature for 1 h. The liquid was collected and centrifuged at 8000 rpm for 15 min at room temperature. The supernatant containing the bacteriophage was used as a stock solution (typical MS2 concentration = 10^{10} PFU/mL) and stored at 4 ℃ before use.

2.3 Bacteriophage Inactivation by Ag and ZnO NPs inferred from the Double Agar Layer Assay (DAL)

To determine bacteriophage inactivation by Ag NPs and ZnO NPs, aliquots of 50% AgNPs and ZnO NPs stock suspension were added into 100 μl of the MS2 stock solution to obtain the final total Ag concentrations of 1, 3, 5 mg/L and the total ZnO concentrations of 5, 10, 20 mg/L, respectively, with samples containing only MS2 stock solutions served as the control. After exposure to nanoparticles (Ag and ZnO NPs) at room temperature for 1 h, the phage samples prepared in triplicate were serially diluted (10-fold) in 1× PBS during the DAL assay (Figure 1). The plates were incubated at 37 ℃ for 6 ~ 8 h and only samples with PFU number ranging from 0 to 300 were enumerated. A separate experiment was carried out to compare the degree of phage inactivation by different silver components (Ag^+ ions, 50% AgNPs and 100% AgNPs) at the same total Ag concentration (5 mg/L).

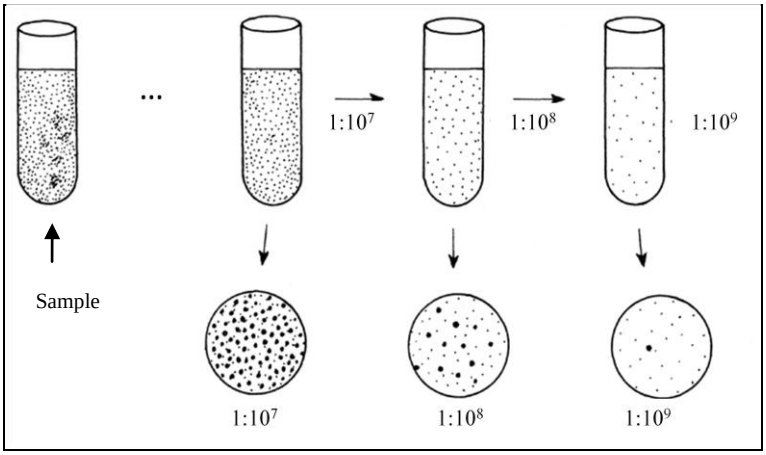

Figure 1. Phage sample preparation with a 10-fold serial dilution

2.4 Bacterial and Bacteriophage Inactivation by Ag and ZnO NPs inferred from the Turbidimetric Microtiter Assay

Samples of pure *E. coli* and a mixed culture containing *E. coli* and bacteriophage MS2 (*E. coli*–MS2 binary system) were prepared in triplicate in the same 96-well microplate for bacterial growth comparison purposes (Figure 2). To prepare the samples, aliquots (10 µl) of an overnight *E. coli* culture (typical cell concentration = 10^8 CFU/ mL) were pipetted into each test well, followed by the addition of 10 µl PBS or 10 µl MS2 for pure *E. coli* culture or *E. coli*–MS2 binary system, respectively. Next, in addition to the blank (nutrient only), positive control (nutrient plus *E. coli*) and the control (nutrient plus *E. coli* and MS2), a known volume of 50% AgNPs or ZnO NPs stock suspensions was added to obtain a series of final concentrations of total Ag (1, 3, 5 mg/L) or ZnO (5, 10, 20 mg/L). Then a corresponding volume of sterilized fresh LB was added to reach a total volume of 210 µl in each test well. The plate was incubated for 1 h at room temperature. A computer program was set up to provide vigorous mixing for 5 s before optical density (OD) was automatically measured at a wavelength of 490 nm once every 1 h using a microreader (VICTOR^3, PerkinElmer, Shelton, USA). A plot of absorbance (OD_{490nm}) against time was used to determine the specific bacterial growth rate (µ), which was calculated via least-squares error analysis (See section 2.5).

Analogous to the experiments during the DAL assay, the same procedure was performed to compare the degree of bacterial growth inhibition by different silver components (Ag^+ ions, 50% AgNPs and 100% AgNPs) at the same total Ag concentration (5 mg/L) under two different bacteriophage MS2 concentrations (low concentration =10^8 and high concentration =10^{10} PFU/mL, respectively).

To actually determine the real bacterial cell numbers and phage numbers, a parallel enumeration study was carried out during the microtiter experiment. The bacterial/phage samples exposed to 100% AgNPs or ZnO NPs at the concentration of 5 mg/L were taken at a predetermined time (1, 6, 11, 24 h) for *E. coli* and MS2 enumeration based on standard agar plate assay and DAL assay, respectively. Particularly for MS2 enumeration during the DAL assay, the mixed bacterial/phage samples were filtered through 0.22 μm filter to remove bacterial cells to avoid interference from the bacteria in the mixed bacterial/phage samples.

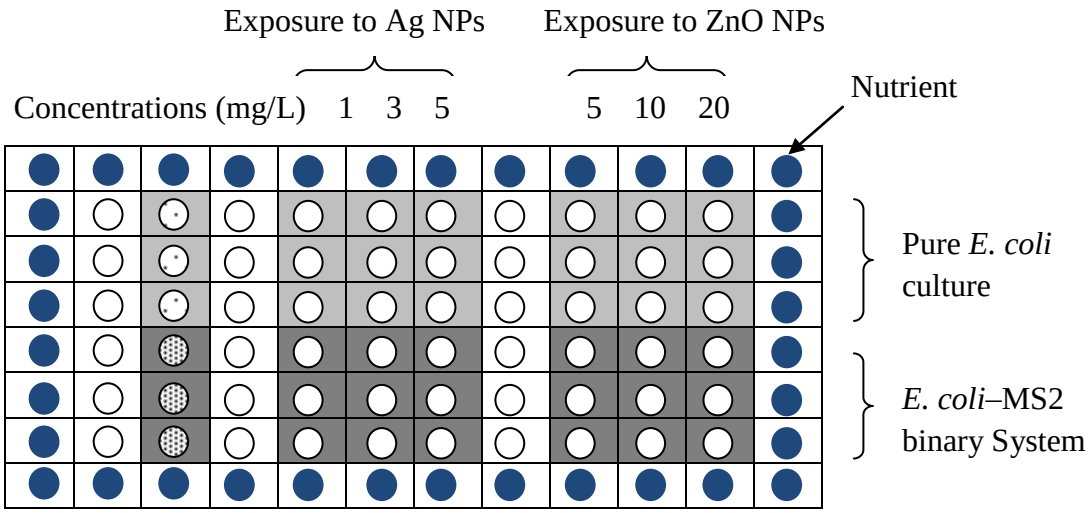

Figure 2. Set-up of a 96-well microplate with samples exposed to different concentrations of 50% AgNPs and ZnO NPs

= nutrient & *E. coli* = nutrient, *E. coli* & MS2

2.5 Determination of specific bacterial growth rate μ (h^{-1})

As one important parameter indicating the growth condition of bacterial community, the specific bacterial growth rate μ was obtained by fitting the experimental data collected during the bacterial exponential growth phase into an exponential growth model (Equation 2).

$$X = X_0 e^{\mu t} \qquad \text{(Equation 2)}$$

Where X = final biomass concentration

X_0 = initial biomass concentration

Both X and X_0 were inferred from the optical density measurements (490 nm). The specific growth rate μ was determined through the least-square error (LSE) analysis via the Microsoft Excel SOLVER function (Choi et al. 2008).

CHAPTER 3 RESULTS

3.1 Characterization of Ag and ZnO NPs

The freshly prepared Ag NP stock suspensions (50% AgNPs and 100% AgNPs at concentration of 0.7 mM) have an average particle size of 15 to 21 nm (via TEM analysis) and were well characterized (Figure 3a and 3b) as described earlier (Choi et al. 2008; Choi et al. 2008). The particle size distribution analysis of nanosilver by TEM (Figure 3c) was generally consistent with those by dynamic light scanning (DLS) (Figure 3d), which indicated that the particle size of the suspension of 100% AgNPs was slightly larger than that of suspension containing 50% AgNPs.

Both ZnO NPs of dry and wet state were characterized in this research work, with physical/chemical properties analysis (Table 3). The true average particle size of ZnO NP suspension determined by TEM was 39 ± 10 nm, with a wide size ranging from 10 to 200 nm (Figure 4). The average particle size was larger than the advertised size (20 nm). The size discrepancy was likely caused by particle aggregation during the drying process, as similar phenomenon had been reported in other studies (Adams et al. 2006; Zhang et al. 2007).

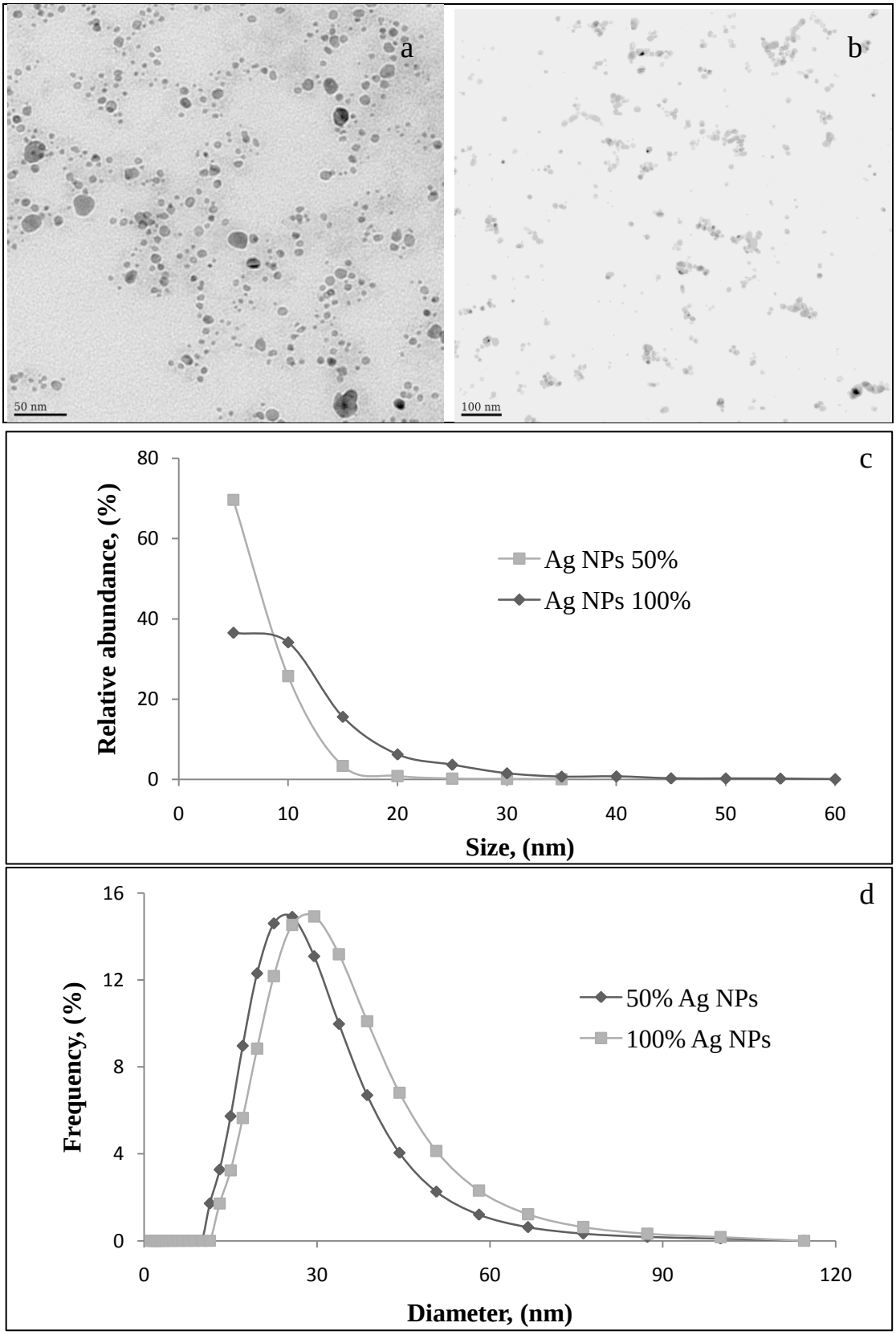

Figure 2. Particle size analysis using TEM and DLS for Ag NPs

TEM images of 50% AgNPs (50:50 of Ag^{+}/nanosilver in mass ration) (a) (scale bar = 50 nm) and 100% AgNPs (b) (scale bar = 100 nm). (c) Size distributions of 50%

AgNPs and 100% AgNPs. (d) Particle size analysis of 50% AgNPs (primary particles size = 25 nm) and 100% AgNPs (primary particle size = 29 nm) by dynamic light scattering (DLS).

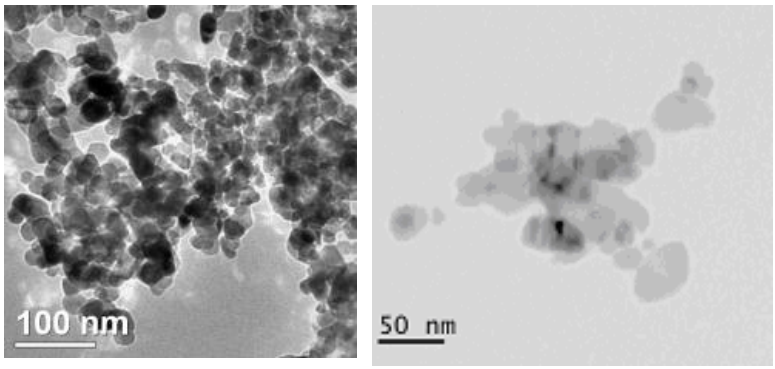

Figure 3. Size characterization of ZnO NPs

TEM images of ZnO NPs in dry (left panel) and wet state (right panel) (average particle size = 39 nm, scale bar = 50 nm).

Table 3. Physical/chemical properties of the ZnO NPs.

	reported primary particle size (nm) by supplier	surface area (m^2/g)	area density (g/cm^3)	calculated size in dry state (nm)	Purity
ZnO NPs	20	50	5.6	21	99.5%

3.2 Bacteriophage Inactivation by Ag NPs Inferred from the DAL Assay.

As can be seen in Fig 5a, the number of bacteriophage did not decrease with exposure to the 50% AgNPs suspension as the total Ag concentration increased from 0 to 5 mg/L Ag. Student t-test based on ANOVA analysis indicated that there was no significant difference (Table 4) in MS2 plaque numbers before and after phage

exposure to 50% AgNPs if the concentration of total Ag was below 5 mg/L. The result is consistent with earlier studies showing that at the concentration of 12.5 mg/L Ag, the non-coated or polysaccharide-coated Ag NPs (particle sizes from 25 to 80 nm) neither increased nor decreased monkeypox virus (MPV) plaque formation (Rogers et al. 2008). It was demonstrated that the nAg-PSF membranes (silver nanoparticles impregnated polysulfone ultrafiltration membranes) seldom reduced the number of bacteriophage MS2 (Zodrow et al. 2009).

In the parallel experiment based on the antiviral activities of different silver components on phage MS2, similar results were observed for both Ag^+ ions and 100% AgNPs at the total concentrations of 5 mg/L Ag (Figure 5b). The insignificant difference obtained for the four groups studied (Table 5) demonstrates that at a total silver concentration of 5 mg/L and below, neither pure nanosilver, Ag^+ ions, nor the mixture of nanosilver and Ag^+ ions could deactivate bacteriophage MS2.

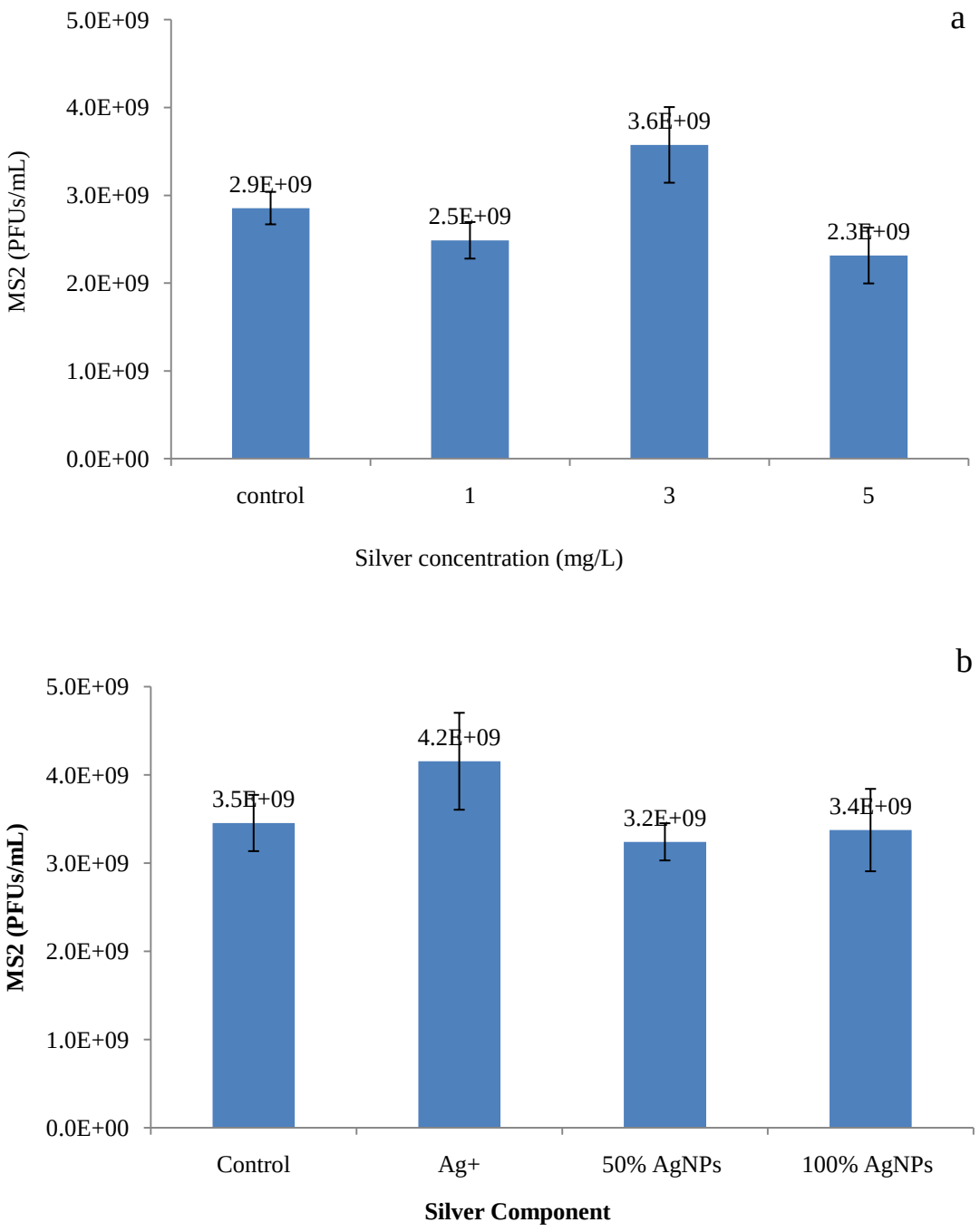

Figure 4. Bacteriophage MS2 inactivation by Ag NPs

Bacteriophage MS2 number changes after 1 h exposure to 50% AgNPs at different total silver concentrations (a) and to different silver components at the same total Ag concentration (5 mg/L) (b).

Table 4. ANOVA analysis of the inhibitory effect of 50% AgNPs at different concentrations on bacteriophage MS2 inferred from

	Compared with control		
50% AgNPs	1 mg/L	3 mg/L	5 mg/L
P-value	0.085	0.056	0.064

Table 5. ANOVA analysis of the inhibitory effect of different silver components at the total concentration of 5 mg/L Ag on bacteriophage MS2

	Compared with the control			50% vs 100% AgNPs
Different silver components (5 mg/L)	Ag^+	50% AgNPs	100% AgNPs	
P-value	0.129	0.388	0.060	0.676

3.3 Bacteriophage Inactivation by ZnO NPs Inferred from the DAL Assay

As presented in Figure 6, almost the same MS2 number as the control was observed when exposed to ZnO NPs at the total concentration of 5 or 10 mg/L ZnO, which was confirmed by ANOVA analysis (Table 6). However, samples treated with 20 mg/L ZnO NPs resulted in much higher plaque numbers than the other groups. The result has a statistically significant difference (P-value = 0.04) indicating that ZnO NPs might help bacteriophage MS2 to grow better at a total concentration of 20 mg/L ZnO.

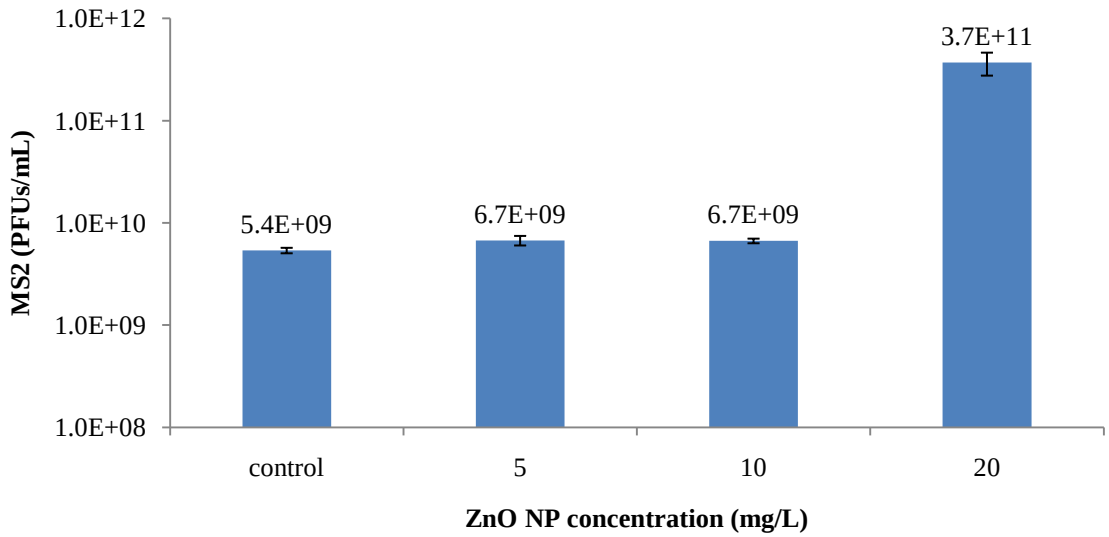

Figure 5. Bacteriophage MS2 number changes after a 1h exposure to ZnO NPs at different concentration using the standard DAL method

Table 6. ANOVA analysis of the inhibitory effect of ZnO NPs on bacteriophage MS2 (student t-test)

	Compared with control		
ZnO NPs	5 mg/L	10 mg/L	20 mg/L
P-value	0.060	0.106	0.040

3.4 Bacterial and Bacteriophage Inactivation by Ag NPs Inferred from the Microtiter Assay

Based on the microtiter assay, a plot of optical density (490 nm) versus time was obtained as the bacterial growth curve. In the pure *E. coli* system, 50% AgNPs inhibited *E. coli* growth, which is reflected in the parameters inferred from the bacterial growth curve (Figure 7a). At total silver concentrations of 0, 1, 3 and 5 mg/L, (1) the lengths of the lag phase of the bacterial growth were 1, 3, 4.5 and 6

hours, respectively; (2) the corresponding bacterial specific growth rates μ (section 2.5) were 0.171 ± 0.008, 0.123 ± 0.004, 0.049 ± 0.019 and 0.032 ± 0.01, respectively; (3) the maximum ODs (the maximum value of optical density when bacterial growth reach the stationary phase) were 0.615 ± 0.011, 0.556 ± 0.050, 0.525 ± 0.001 and 0.487 ± 0.021, respectively. As the total concentration of 50% AgNPs increased from 1 to 5 mg/L of Ag, the trend of increasing lag phase length combined with decreasing specific bacterial growth rate μ and maximum ODs all indicated the inhibitory behavior of 50% AgNPs on *E. coli*. These results were consistent with previous studies demonstrating that even at low concentrations of Ag NPs, *E. coli* exhibit a long adaptation time, coupled with bacterial growth inhibition (Sondi et al. 2004; Choi et al. 2008).

In the system containing both *E. coli* and bacteriophage MS2, a similar pattern of initial bacterial growth curve and same length of lag phase were observed for the bacteria/phage binary system being exposed to 50% AgNPs (Figure 7b). As bacteria grew, bacteriophage proliferation and reproduction likely resulted in the release of more MS2 for bacterial infection reaches a pesudo-stationary growth phase (almost flat line between hour 8 and 13, Figure 7b). In the presence of 50% AgNPs, however, a decrease of optical density (starting from about hour 10 to 15) became evident, indicating the occurrence of *E. coli* cell lysis. This was supported by a parallel active bacteria and phage number study showing the substantial growth of MS2 after a few hours of incubation (Table 7). Meanwhile, compared with the control, the optical

density of the samples treated with 50% AgNPs decreased with a more evident and sharp trend, which might be due to AgNP promoted bacteriophage infection on *E. coli* resulting in cell lysis and reduced OD values.

To evaluate the viral activity in the *E. coli*–MS2 binary system, several parameters inferred from the bacterial growth curve were determined and compared.

(1) Delta time (Δt), defined as the time difference between the end point of lag phase period and the reflection point (the point at which OD value started to decrease, as marked on Figure 7c), might serve as another indicator of the MS2 activity in the presence of 50% AgNPs. At the total Ag concentrations of 0, 1, 3 and 5 mg/L, the Δt values were 8.8 ± 1.2 h, 8.2 ± 0.3 h, 6.2 ± 0.6 h and 5.8 ± 0.3 h, respectively. As the nanosilver concentration increased from 1 to 5 mg/L of Ag, the decreasing trend in Δt implied that bacteriophage might infect the bacterial hosts more easily or rapidly in the presence of 50% AgNPs.

(2) Specific growth rate (μ). Regardless of the nanosilver treatment, bacteria started to grow again and reached the maximum ODs (Figure 7b). However, the bacterial growth rates in the *E. coli*-MS2 binary system were reduced to 0.045 ± 0.003, 0.036 ± 0.001, 0.026 ± 0.002, and 0.021 ± 0.001 at 0, 1, 3, and 5 mg/L total Ag, respectively, which were significantly lower than those in pure *E. coli* system (P-value < 0.05). The

reduced growth rates indicated a strong detrimental effect of MS2 on *E. coli* growth in the presence of nanosilver, although *E. coli* could still grow by retaining MS2 inside the cell to produce phage-resistant bacteria cells or repairing its damaged membrane due to phage infection (Rishi et al. 2006).

(3) Delta optical density (ΔOD), defined as the OD value difference of the pure *E. coli* system and the *E. coli*/MS2 binary system when treated with the same concentration of nanosilver (Figure 7d). Regardless of the nanosilver treatment, bacterial growth eventually reached the stationary phase as evidenced by a maximum OD value (Figure 5b). Due to bacteriophage infection, the maximum ODs for all treatments of the *E.coli*-MS2 binary system were lower than those of the pure E. coli system. Delta OD (Δ OD, the difference of the maximum OD values between the two (pure vs. binary) systems with exposure of the same concentrations of nanosilver) was considered to be the result of MS2 infection. At total concentrations of 50% AgNPs of 0, 1, 3 and 5 mg/L Ag, the ΔOD values were 0.088 ± 0.004, 0.104 ± 0.003, 0.134 ± 0.008 and 0.126 ± 0.017, respectively. Earlier studies suggest that the RNA phage MS2 is generally unable to cause lysis of *E. coli* cells when they are approaching or in stationary phase (Haywood 1974), the positive relationship of ΔOD values and 50% AgNPs concentrations indicated that nanosilver might help bacteriophage infect the bacteria host at the concentrations tested in this study.

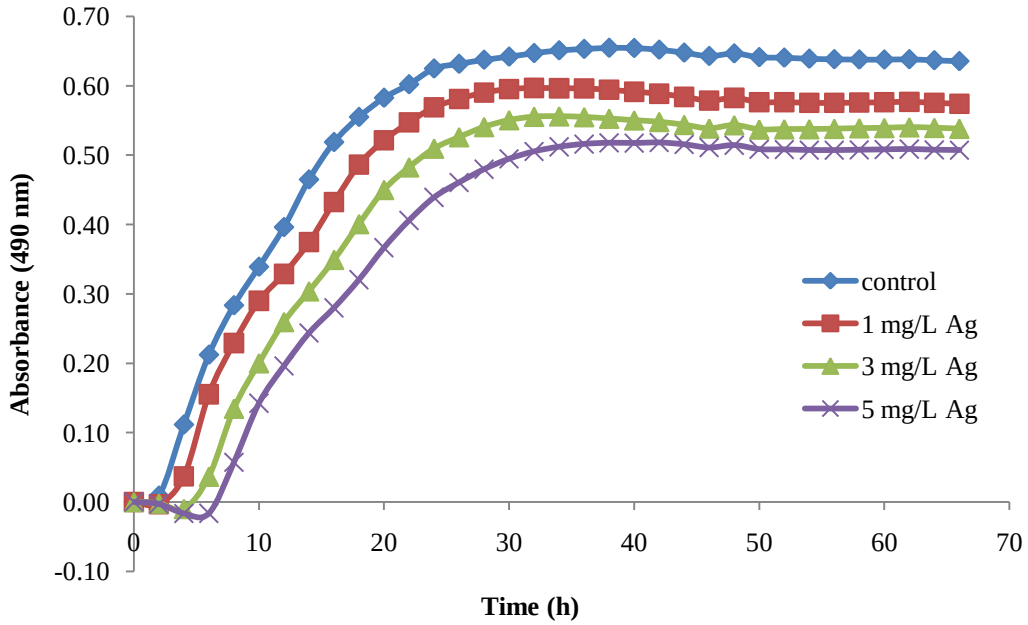
a
Absorbance (490 nm)
0.70
0.60
0.50
0.40
0.30
0.20
0.10
0.00
-0.10
0
10
20
30
40
50
60
70
Time (h)
control
1 mg/L Ag
3 mg/L Ag
5 mg/L Ag

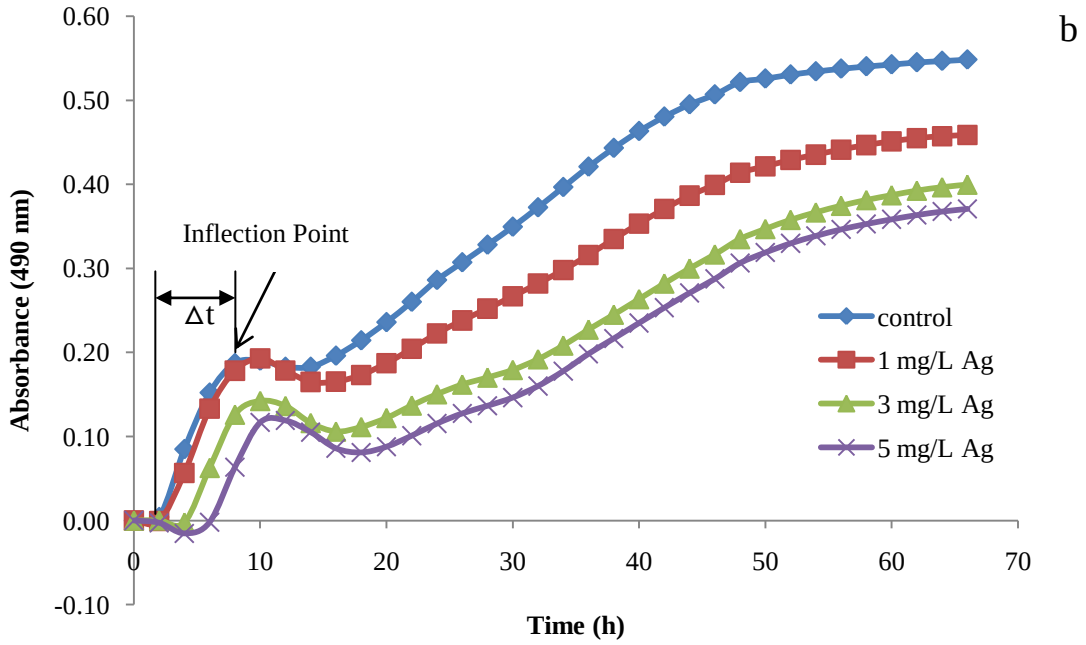
b
Absorbance (490 nm)
0.60
0.50
0.40
0.30
0.20
0.10
0.00
-0.10
Inflection Point
Δt
0
10
20
30
40
50
60
70
Time (h)
control
1 mg/L Ag
3 mg/L Ag
5 mg/L Ag

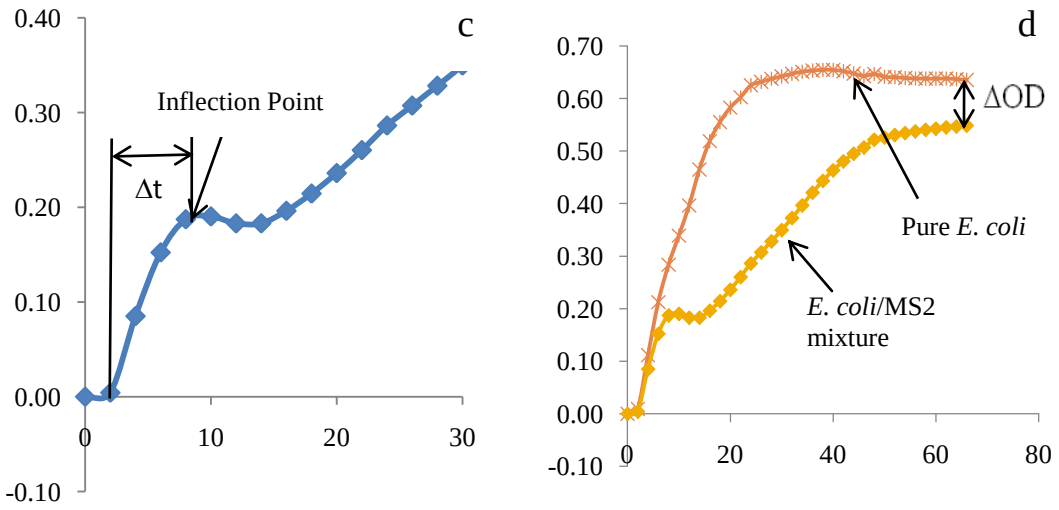

Figure 6. Bacterial growth in the presence of 50% AgNPs (total Ag concentration ranges from 0 to 5 mg/L) in the pure *E. coli* system (a) and the *E. coli*-MS2 binary system (b) inferred from the turbidimetric microtiter assay.

Illustration of Δt (c) and ΔOD (d).

Table 7. Time course change of bacterial and bacteriophage number in a mixture of *E. coli* and MS2 after exposure to 100% AgNPs (5 mg/L) or ZnO NPs (20 mg/L) inferred from the standard agar plate and double agar layer assay, respectively

	Treatments	1 h	6 h	11 h	24 h
E. coli (CFUs/mL)	AgNPs	7.1E+06	1.4E+07	5.0E+06	4.3E+07
	ZnO NPs	7.5E+06	4.3E+07	6.3E+06	1.2E+07
	Ctrl*	1.1E+07	4.6E+07	5.5E+07	7.0E+07
MS2 (PFUs/mL)	AgNPs	9.3E+11	4.2E+11	1.1E+18	2.6E+18
	ZnO NPs	2.6E+13	9.5E+14	2.0E+20	1.8E+21
	Ctrl*	1.4E+08	7.3E+09	1.2E+15	1.1E+15

* Ctrl refer to as the *E. coli* – MS2 binary system

3.5 Bacterial and Bacteriophage Inactivation by ZnO NPs Inferred from the Microtiter Assay

In general, similar bacteria and bacteriophage inactivation patterns were observed when the pure *E. coli* or *E. coli*-phage system was exposed to ZnO NPs with only a few changes. First, at concentrations of 0, 5 and 10 mg/L ZnO, similar bacterial growth profiles and length of lag phase period (about 2h) were observed in the pure *E. coli* system, indicating no bacterial growth inhibition occurred at ZnO concentrations of 10 mg/L or below. In the presence of 20 mg/L ZnO NPs, however, the bacterial growth curve eventually deviated from the control (Figure 8a). The final OD values were 0.615 ± 0.011, 0.605 ± 0.012, 0.595 ± 0.013, 0.591 ± 0.012 for samples treated with ZnO NPs at the concentrations of 0, 5, 10, and 20 mg/L ZnO respectively, indicating slight bacterial growth inhibition at the ZnO NPs concentration of 20 mg/L ZnO. The results were consistent with other studies suggesting that bacterial growth inhibition only occur at a much higher concentration of ZnO NPs (Adams et al. 2006; Jones et al. 2008; Y. Liu 2009), although ZnO NPs could display more significant antibacterial action at the lower initial *E. coli* concentration (Pal et al. 2007) .

In the bacteria/phage binary system, there was no significant difference of the length of lag phase periods among the four treatments (Figure 8b). However, at the concentrations of 5, 10 and 20 mg/L ZnO, all Δt values (as defined in section 3.4) were reduced to 4 h, 2 h less than that of the control (Figure 8b). Moreover, a rapid

OD decrease was detected after 6 hours of incubation in the presence of ZnO NPs regardless of the concentration. These results suggested again that ZnO NPs did not inhibit MS2 growth. Instead, ZnO NPs might help MS2 infect *E. coli* more easily, which was confirmed from a parallel active bacteria and phage number study showing a substantial growth increase of MS2 after 6 h incubation (Table 7).

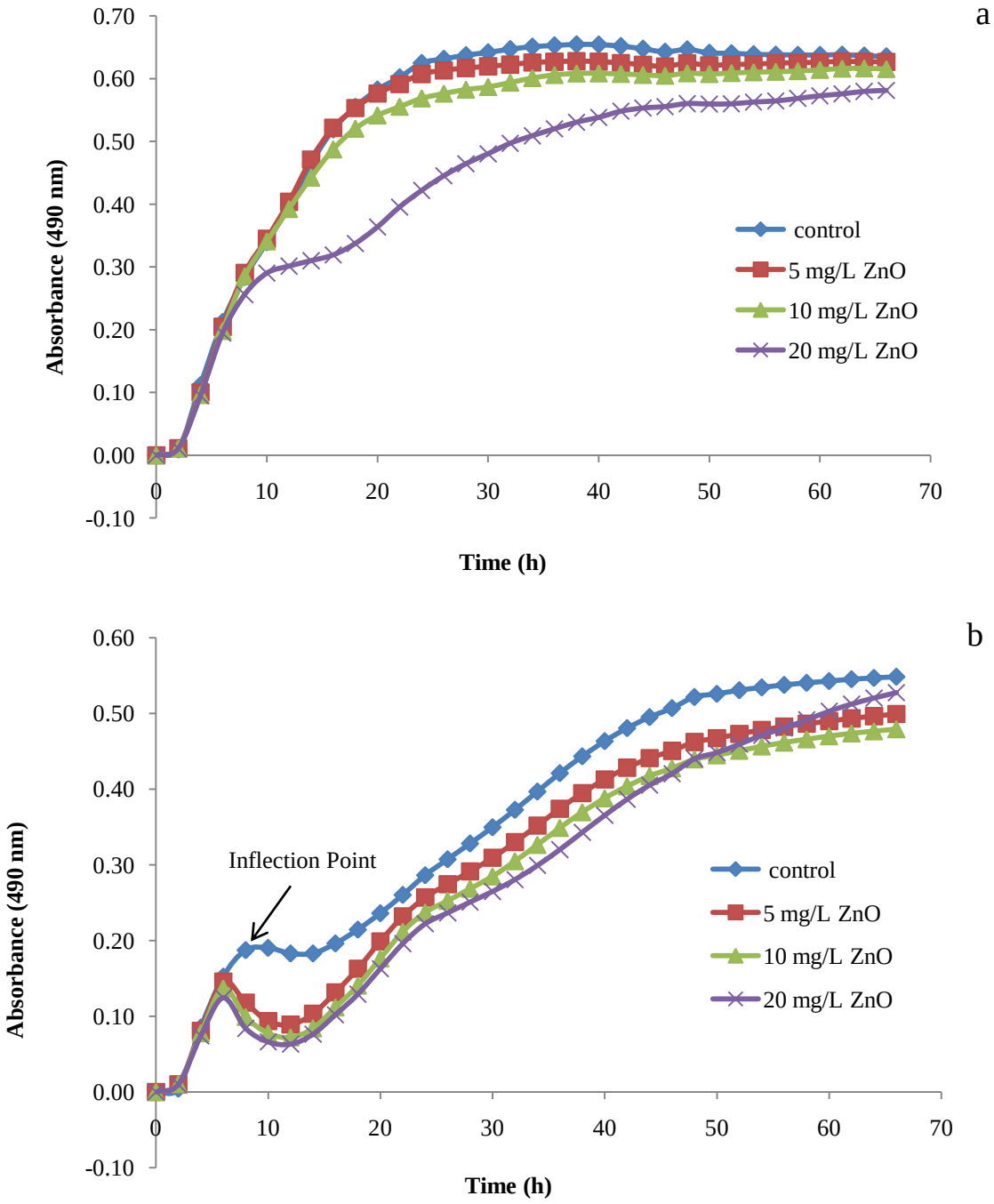

Figure 7. Bacterial growth in the presence of ZnO NP (total ZnO concentration ranges from 0 to 20 mg/L) in the pure *E. coli* system (a) and the *E. coli*-MS2 binary system (b) inferred from the turbidimetric microtiter assay

3.6 Time course change of bacterial and bacteriophage number

A parallel study of the time course change of bacterial cell number and bacteriophage number in the mixed *E. coli*/MS2 samples was carried out to track bacterial/phage growth. The standard agar plate and DAL methods were applied to determine the true bacterial cell and bacteriophage number (Table 7) during the turbidimetric based bacterial/phage growth assay (Figure 9). Not surprisingly, the patterns of the changes in bacterial cell numbers (Table 7) were consistent with those from the turbidimetric microtiter assays (Figures 7-9).

It is important to note that the MS2 numbers increased after a short period of incubation in all nanoparticle treated samples and the control, reaching a plateau at about 24 h incubation (Table 7). For the control sample containing only *E. coli* and MS2, the result was consistent with that from the turbidimetric based assay showing that the *E. coli* number was relative constant between incubation hour 5 and 11 . For the mixed *E. coli*/MS2 samples treated with 100% AgNPs and ZnO NPs, the MS2 numbers (in PFUs) were approximately 3 and 5 orders of magnitude higher than those of the control, strongly suggesting that both nanoparticles facilitated MS2 to infection of the *E. coli* host cells.

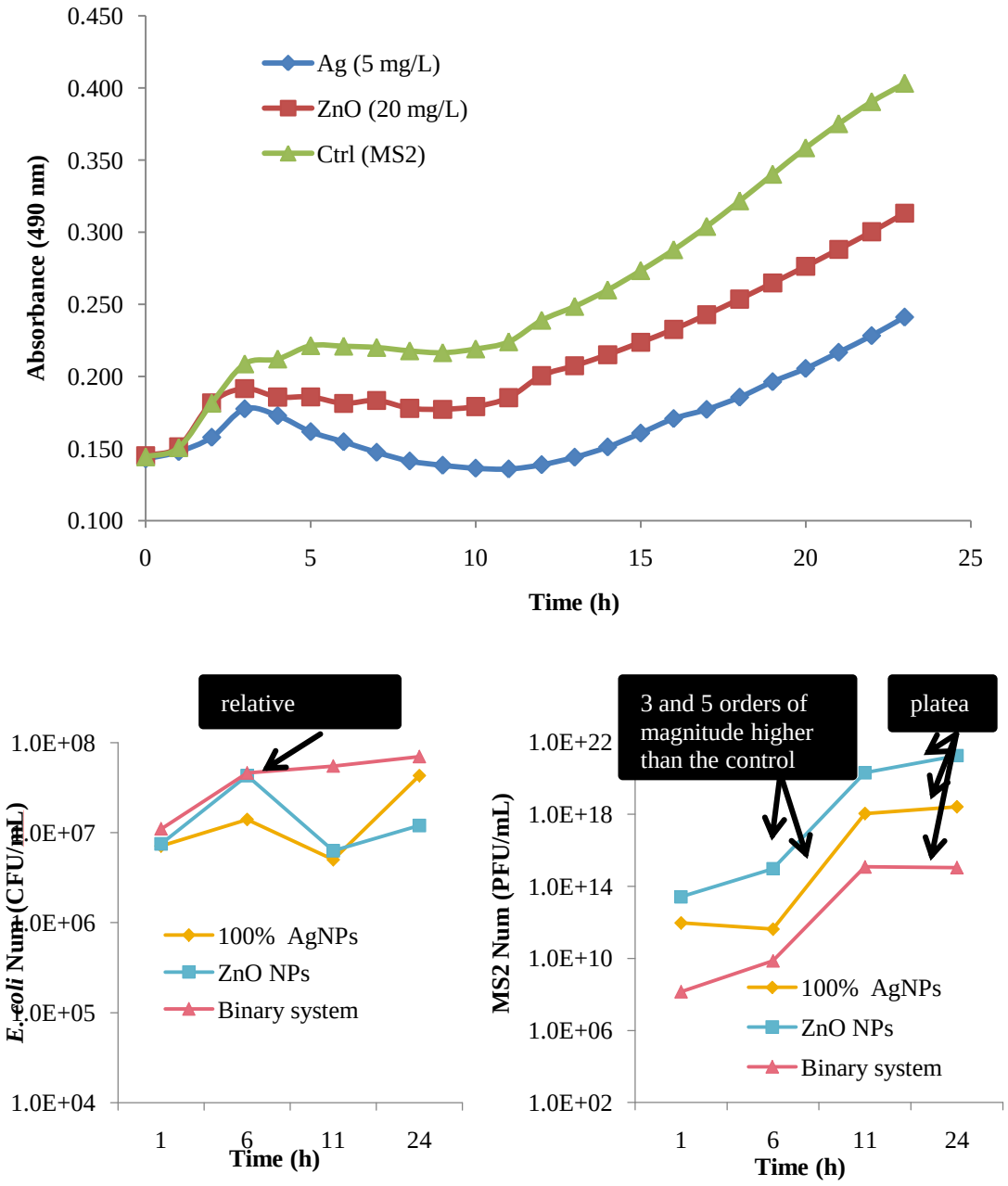

Figure 8. Bacterial growth in the presence of 100% AgNPs (5 mg/L) and ZnO NPs (20 mg/L) inferred from the turbidimetric microtiter assay (control samples contain *E. coli* and MS2 only)

This experiment was carried out in parallel to the agar-based bacterial and phage enumeration study (results presented in Table 7).

3.7 Bacterial and Bacteriophage Inactivation by Different Silver Components at Low and High Phage Concentrations

At low bacteriophage MS2 concentrations (around 10^8 PFU/ mL), the bacterial growth curve in the *E. coli*–MS2 system overlapped with that from the pure *E. coli* system (Figure 10a), showing minimal inhibition of phage MS2 against *E. coli* growth. Compared with the control, similar patterns of growth curve were obtained for the mixed *E. coli*/MS2 samples treated with 50% AgNPs and 100% AgNPs (Figure 10a). Of all the silver treated samples (final total Ag concentration = 5 mg/L), Ag^+ ions exhibited the highest toxicity, resulting in complete inhibition on *E. coli* throughout the test. Although the same maximum OD values were observed for samples treated with both nanosilver suspensions (100% and 50% AgNPs), 100% AgNPs appeared to be more toxic than the 50% AgNPs, as reflected by a longer lag phase (14 h Vs 4 h). This result could be assumed to the slow and continuous release of Ag^+ ions from Ag NPs (Choi et al. 2008; Navarro et al. 2008).

At the high bacteriophage MS2 concentrations (around 10^{10} PFU/ mL), the bacterial growth curve derived from the *E. coli*/MS2 systems was differed from that for the pure *E. coli* system (Figure 10b), indicating a significant bacterial infection by MS2. Analogues to the result from the low initial bacteriophage concentration study, Ag^+ ion (5 mg/L of total Ag) completely inhibited bacterial growth throughout the test, demonstrating the strong antibacterial property of Ag^+ ions. In the presence of 50%

AgNPs at 5 mg/L total Ag, the bacterial growth curve exhibited the same pattern as demonstrated in Figure 7, which indicated bacterial growth after a short lag phase period to reach a pseudo stationary phase and later started to increase again, indicating the complex interactions among MS2, 50% AgNPs and bacteria. Although similar patterns of bacterial growth curves were observed for *E. coli*/MS2 samples treated with 50% AgNPs and 100% AgNPs, 50% AgNPs appeared to be more toxic than 100% AgNPs (Figure 10b).

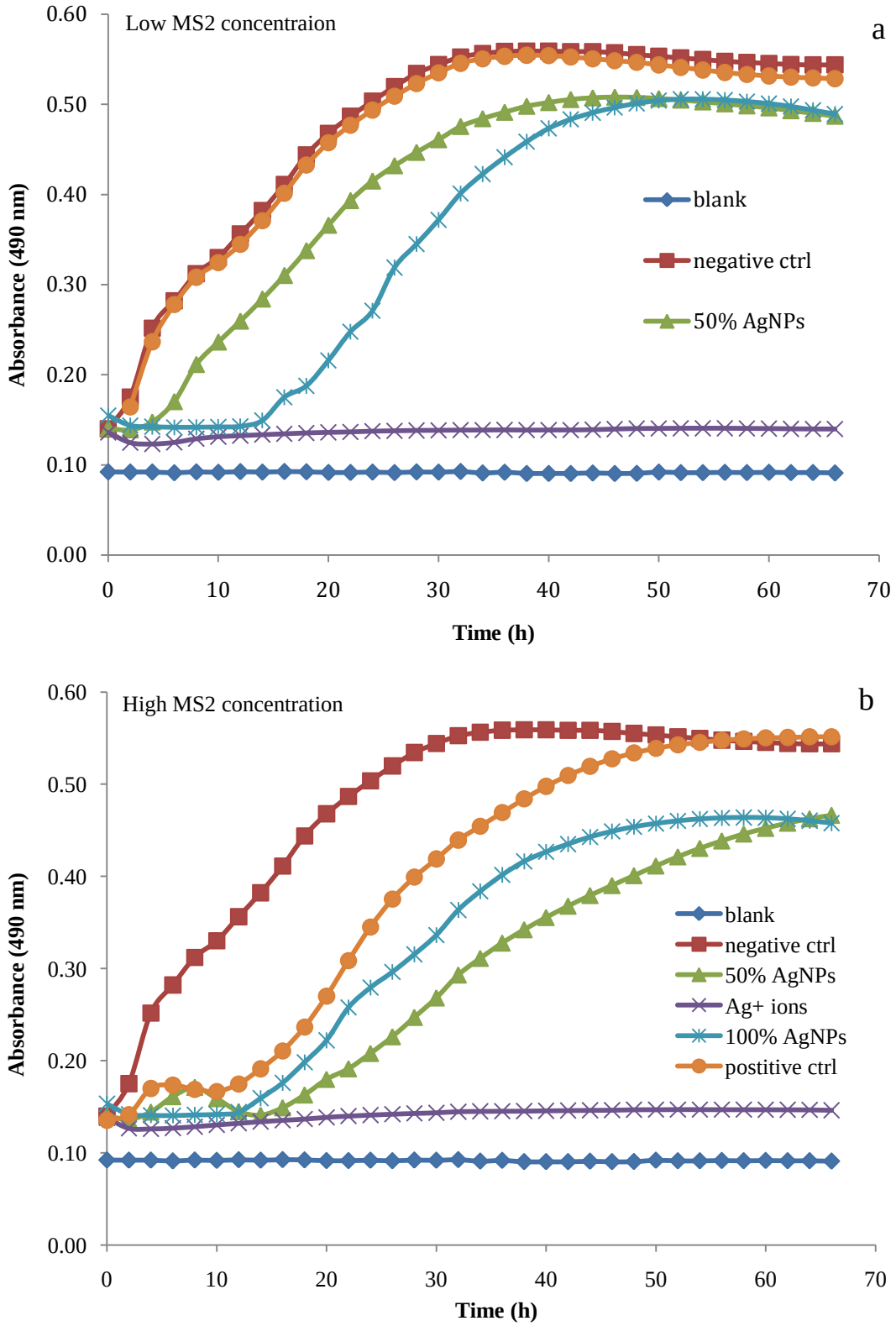

Figure 9. Bacterial growth in the presence of different silver component (Ag^+ ions (×), 50% AgNPs (▲) and 100% AgNPs (*)) at low MS2 concentration (10^8 PFUs/mL) (a) or high MS2 concentration (10^{10} PFUs/mL) (b)

All samples had the same total Ag concentration (5 mg/L). Blank (♦) refer to as samples containing nutrient media only; negative control (■) refer to as samples containing *E. coli* only; positive control (●) refer to as samples containing both *E. coli* and MS2.

CHAPTER 4 DISCUSSIONS

Studies on the inhibitory behaviors of nanoparticles on microbial communities such as bacteria and viruses are important but challenging (Choi et al. 2008; Shirasaki et al. 2009), because viruses as unable to reproduce or proliferate outside a host cell, and also due to the involvement of the complex interactions among bacteria, bacteriophage and nanoparticles.

Although the mechanism of cell lysis caused by single-stranded RNA bacteriophage (e.g., MS2) infection is still not completely understood, it is generally agreed that MS2 could cause bacterial cell lysis by destroying the structure of cell membrane. Many bacteriophages release their progeny from the former host cells to the new host cells through the action of holins that form lesions in the cytoplasmatic membrane and lysins that degrade the bacterial peptidoglycan (Young 1992; Young et al. 2000; Frias et al. 2009). MS2 phages lyse their bacterial host cells using a low molecular-weight hydrophobic protein that is sufficient to trigger lysis of the host bacteria (Nishihara 2002). Several studies also show that the phage L-protein reacts with the inner and outer membrane systems to release endogenous murein hydrolases (Holtje et al. 1988).

As demonstrated in other studies, the inhibitory effect of Ag NPs on host bacterial growth could result from the damage of host cell wall and membrane system and the

increase of cell membrane permeability (Sondi et al. 2004; Lok et al. 2006; Choi et al. 2008; Nair et al. 2008). Many metal oxide nanoparticles have similar actions to change bacterial cell properties (Stoimenov et al. 2002; Adams et al. 2006; Zhang et al. 2007). Electron microscopic analyses have shown that ZnO nanoparticles damage the bacterial cell wall (Adams et al. 2006; Zhang et al. 2007) and cause an increase of *E. coli* membrane permeability leading to accumulation of ZnO NPs in the cell membrane and nanoparticle internalization (Brayner et al. 2006).

On the contrary, bacteriophage MS2 are less sensitive to Ag or ZnO NPs than bacteria. Recent studies presented similar findings that 4-log inactivation of *E. coli* was achieved after 5 min exposure to UV while no inactivation occurred with MS2 under the same conditions (Badireddy et al. 2007). The mechanism behind the inactivation or inhibition of phage function by NPs is not studied in this work. However, it is clear from our study that bacteria are more sensitive to nanosilver inhibition than MS2 phages.

We demonstrated that Ag NPs and ZnO NPs might help facilitate bacterial infection resulting in a several orders of magnitude increase of bacteriophage numbers (Table 7). As observed in Figure 10, there is slight difference for the toxicity profiles of 50% AgNPs and 100% AgNPs at different initial bacteriophage concentrations (Figure 10). Several reasons associated with the slow release of Ag^+ ions from nanosilver (Choi et al. 2008) might be responsible for the difference. First, at high initial bacteriophage

concentrations, MS2 might cause faster and more intensive infection of the *E. coli* cell hosts, which likely resulted in a rapid membrane property change and dysfunction to allow Ag^+ ions to enter the cell more easily. In this case, the Ag^+ ions in 50% AgNPs could immediately interact with bacteria to inhibit *E. coli* more easily compared with the slow release of Ag^+ ions from 100% AgNP suspension. Other reasons could be due to the development of phage resistant bacteria. More phage resistant bacteria might exist in the presence of high bacteriophage MS2 concentration to handle the continuous release of Ag^+ ion from nanosilver which thereby less affected by the toxicity of 100% AgNPs (Rishi et al. 2006).

CHAPTER 5 CONCLUSIONS

The inhibitory action of silver and zinc oxide nanoparticles on bacteria and viruses were evaluated. *E. coli* and bacteriophage MS2 were selected as the model microorganisms for bacteria and bacteriophage, respectively. Both silver and zinc oxide nanoparticles were prepared and characterized before use. The numbers of both *E. coli* and phage MS2 were determined by enumeration in traditional agar plate based methods and inferred from automatic turbidimetric microtiter assays.

Ag NPs caused substantial *E. coli* growth inhibition at concentrations of 5 mg/L Ag and below). Compared to Ag NPs, ZnO NPs demonstrated a much lower degree of inhibition against *E. coli* and only ZnO NPs at a concentration of 20 mg/L resulted in slight inhibition of bacterial growth.

Both nanoparticles failed to deactivate bacteriophage MS2 at the highest test concentration (5 mg/L Ag and 20 mg/L ZnO). Instead, exposure to 20 mg/L ZnO NPs seemed facilitate MS2 growth, as evidenced by the much higher plaque numbers obtained from the DAL assay. Both Ag^{+} ions and nanosilver suspensions (at the total concentration of 5 mg/L Ag) did not result in virus inactivation.

In the *E. coli*/MS2 binary system, both phage MS2 and silver containing chemicals contributed to the inhibition of *E. coli* growth, although the degree of inhibition appeared to be depended on initial phage concentration. Ag^{+} ions at concentration of 5 mg/L inhibited the growth of *E. coli* completely.

Rather than inhibiting the virus growth, both nanoparticles seemed to facilitate the infection of bacteriophage MS2 in the *E. coli* host, as supported by the parallel agar-based enumeration test of bacterial and MS2 growth.

In summary, nanosilver exposure resulted in a decrease in *E. coli* growth rates, which are likely coupled with the bacteriophage infections. It is speculated that the formation of "pits" on the bacterial cell wall and membrane permeability increase that resulting from nanoparticle exposure may help the virus enter or leave the cell more easily. The changes of bacterial cell structure and increasing membrane permeability because of nanoparticle exposure might help cell lysis by bacteriophage and MS2 growth, as demonstrated during the turbidimetric microtiter assay and the standard double agar layer assay, respectively. By monitoring the dynamic bacterial growth through the automatic and less labor intensive microtiter method, more insightul information on bacterium-virus interactions can be obtained and possibly used for mathematical modeling of the dynamics of viral infections (Campos et al. 2008). This research work

will help to better understand the adverse effect of the commercially available nano-products on the natural and engineered environment.

REFERENCE

Adams, L. K., D. Y. Lyon, et al. (2006). "Comparative eco-toxicity of nanoscale TiO2, SiO2, and ZnO water suspensions." Water Research **40**(19): 3527-3532.

Adams, M. H. (1959). *Bacteriophages*. New York, Interscience Publishers.

Amro, N. A., L. P. Kotra, et al. (2000). "High-Resolution Atomic Force Microscopy Studies of the Escherichia coli Outer Membrane: Structural Basis for Permeability." Langmuir **16**(6): 2789-2796.

Amro, N. A., L. P. Kotra, et al. (2000). "High-resolution atomic force microscopy studies of the Escherichia coli outer membrane: structural basis for permeability." Langmuir **16**(6): 2789-2796.

Badireddy, A. R., E. M. Hotze, et al. (2007). "Inactivation of bacteriophages via photosensitization of fullerol nanoparticles." Environmental Science and Technology **41**(18): 6627-6632.

Barry, P. R., P. Peter, et al. (2004). "Long-range absorption enhancement in organic tandem thin-film solar cells containing silver nanoclusters." Journal of Applied Physics **96**(12): 7519-7526.

Becheri, A., M. Dürr, et al. (2008). "Synthesis and characterization of zinc oxide nanoparticles: application to textiles as UV-absorbers." Journal of Nanoparticle Research **10**(4): 679-689.

Behnajady, M. A., N. Modirshahla, et al. (2006). "Kinetic study on photocatalytic degradation of C.I. Acid Yellow 23 by ZnO photocatalyst." Journal of Hazardous Materials **133**(1-3): 226-232.

Birla, S. S., V. V. Tiwari, et al. (2009). "Fabrication of silver nanoparticles by Phoma glomerata and its combined effect against Escherichia coli, Pseudomonas aeruginosa and Staphylococcus aureus." Letters in Applied Microbiology **48**(2): 173-179.

Blattner, F. R., G. Plunkett Iii, et al. (1997). "The complete genome sequence of Escherichia coli K-12." Science **277**(5331): 1453-1462.

Brayner, R., R. Ferrari-Iliou, et al. (2006). "Toxicological Impact Studies Based on Escherichia coli Bacteria in Ultrafine ZnO Nanoparticles Colloidal Medium." Nano Letters **6**(4): 866-870.

Campos, D., V. Mendez, et al. (2008). "The effects of distributed life cycles on the dynamics of viral infections." J Theor Biol **254**(2): 430-8.

Choi, O., K. K. Deng, et al. (2008). "The inhibitory effects of silver nanoparticles, silver ions, and silver chloride colloids on microbial growth." Water Research **42**(12): 3066-3074.

Choi, O. and Z. Hu (2008). "Size Dependent and Reactive Oxygen Species Related Nanosilver Toxicity to Nitrifying Bacteria." Environmental Science & Technology **42**(12): 4583-4588.

Elechiguerra, J. L., J. L. Burt, et al. (2005). "Interaction of silver nanoparticles with HIV-1." Journal of Nanobiotechnology **3**.

Feng, Q. L., J. Wu, et al. (2000). "A mechanistic study of the antibacterial effect of silver ions on Escherichia coli and Staphylococcus aureus." Journal of Biomedical Materials Research **52**(4): 662-668.

Frias, M. J., J. Melo-Cristino, et al. (2009). "The autolysin LytA contributes to efficient bacteriophage progeny release in Streptococcus pneumoniae." J Bacteriol **191**(17): 5428-40.

Gaballa, A. and J. D. Helmann (1998). "Identification of a Zinc-Specific Metalloregulatory Protein, Zur, Controlling Zinc Transport Operons in Bacillus subtilis." J. Bacteriol. **180**(22): 5815-5821.

Gogoi, S. K., P. Gopinath, et al. (2006). "Green fluorescent protein-expressing Escherichia coli as a model system for investigating the antimicrobial activities of silver nanoparticles." Langmuir **22**(22): 9322-9328.

Gun'ko, V. M., J. P. Blitz, et al. (2009). "Structural and adsorption characteristics and catalytic activity of titania and titania-containing nanomaterials." Journal of Colloid and Interface Science **330**(1): 125-137.

Havelaar, A. H., M. Van Olphen, et al. (1993). "F-specific RNA bacteriophages are adequate model organisms for enteric viruses in fresh water." Applied and Environmental Microbiology **59**(9): 2956-2962.

Haywood, A. M. (1974). "Lysis of RNA phage infected cells depends upon culture conditions." Journal of General Virology **22**(3): 431-435.

Henglein, A. (1998). "Colloidal Silver Nanoparticles: Photochemical Preparation and Interaction with O2, CCl4, and Some Metal Ions." Chemistry of Materials **10**(1): 444-450.

Henglein, A. (2002). "Physicochemical properties of small metal particles in solution: "microelectrode" reactions, chemisorption, composite metal particles, and the atom-to-metal transition." The Journal of Physical Chemistry **97**(21): 5457-5471.

Holtje, J. V., W. Fiedler, et al. (1988). "Lysis induction of Escherichia coli by the cloned lysis protein of the phage MS2 depends on the presence of osmoregulatory membrane-derived oligosaccharides." Journal of Biological Chemistry **263**(8): 3539-3541.

Huang, Z., X. Zheng, et al. (2008). "Toxicological Effect of ZnO Nanoparticles Based on Bacteria." Langmuir **24**(8): 4140-4144.

Hui Yang, C. L., Danfeng Yang, et al. (2009). "Comparative study of cytotoxicity, oxidative stress and genotoxicity induced by four typical nanomaterials: the role of particle size, shape and composition." Journal of Applied Toxicology **29**(1): 69-78.

Jiang, W., H. Mashayekhi, et al. (2009). "Bacterial toxicity comparison between nano- and micro-scaled oxide particles." Environmental Pollution **157**(5): 1619-1625.

Jose Ruben, M. and et al. (2005). "The bactericidal effect of silver nanoparticles." Nanotechnology **16**(10): 2346.

Khlebtsov, N. G. and L. A. Dykman (2010). "Optical properties and biomedical applications of plasmonic nanoparticles." Journal of Quantitative Spectroscopy and Radiative Transfer **111**(1): 1-35.

Kim, J. S., E. Kuk, et al. (2007). "Antimicrobial effects of silver nanoparticles." Nanomedicine: Nanotechnology, Biology and Medicine **3**(1): 95-101.

Klasen, H. J. (2000). "A historical review of the use of silver in the treatment of burns. II. Renewed interest for silver." Burns **26**(2): 131-138.

Kumar, R. and H. Münstedt (2005). "Silver ion release from antimicrobial polyamide/silver composites." Biomaterials **26**(14): 2081-2088.

Lok, C.-N., C.-M. Ho, et al. (2007). "Silver nanoparticles: partial oxidation and antibacterial activities." Journal of Biological Inorganic Chemistry **12**(4): 527-534.

Lok, C. N., C. M. Ho, et al. (2006). "Proteomic analysis of the mode of antibacterial action of silver nanoparticles." Journal of Proteome Research **5**(4): 916-924.

Lu, L., R. W. Y. Sun, et al. (2008). "Silver nanoparticles inhibit hepatitis B virus replication." Antiviral Therapy **13**(2): 252-262.

Mühling, M., A. Bradford, et al. (2009). "An investigation into the effects of silver nanoparticles on antibiotic resistance of naturally occurring bacteria in an estuarine sediment." Marine Environmental Research **68**(5): 278-283.

Maynard, A. D., R. J. Aitken, et al. (2006). "Safe handling of nanotechnology." Nature **444**(7117): 267-269.

McDonnell, G. and A. D. Russell (1999). "Antiseptics and Disinfectants: Activity, Action, and Resistance." Clin. Microbiol. Rev. **12**(1): 147-179.

Morones, J. R., J. L. Elechiguerra, et al. (2005). "The bactericidal effect of silver nanoparticles." Nanotechnology **16**(10): 2346-2353.

Nair, S., A. Sasidharan, et al. (2008). "Role of size scale of ZnO nanoparticles and microparticles on toxicity toward bacteria and osteoblast cancer cells." Journal of Materials Science: Materials in Medicine: 1-7.

Nasser, A., D. Weinberg, et al. (1995). "Removal of hepatitis A virus (HAV), poliovirus and MS2 coliphage by coagulation and high rate filtration." Water Science and Technology **31**(5-6): 63-68.

Navarro, E., F. Piccapietra, et al. (2008). "Toxicity of Silver Nanoparticles to Chlamydomonas reinhardtii." Environmental Science & Technology **42**(23): 8959-8964.

Nel, A., T. Xia, et al. (2006). "Toxic potential of materials at the nanolevel." Science **311**(5761): 622-627.

Newman, M. D., M. Stotland, et al. (2009). "The safety of nanosized particles in titanium dioxide- and zinc oxide-based sunscreens." Journal of the American Academy of Dermatology **61**(4): 685-692.

Nicole Jones, B. R., Koodali T. et al. (2008). "Antibacterial activity of ZnO nanoparticle suspensions on a broad spectrum of microorganisms." FEMS Microbiology Letters **279**(1): 71-76.

Nishihara, T. (2002). "Various morphological aspects of Escherichia coli lysis by two distinct RNA bacteriophages." J Gen Virol **83**(10): 2601-2606.

Pal, S., Y. K. Tak, et al. (2007). "Does the Antibacterial Activity of Silver Nanoparticles Depend on the Shape of the Nanoparticle? A Study of the Gram-Negative Bacterium Escherichia coli." Appl. Environ. Microbiol. **73**(6): 1712-1720.

Pan, Z. W., Z. R. Dai, et al. (2001). "Nanobelts of Semiconducting Oxides." Science **291**(5510): 1947-1949.

Raetz, C. R. H. (1990). "Biochemistry of Endotoxins." Annual Review of Biochemistry **59**(1): 129-170.

Ratte, H. T. (1999). "Bioaccumulation and toxicity of silver compounds: A review." Environmental Toxicology and Chemistry **18**(1): 89-108.

Rishi, J., L. K. Andrea, et al. (2006). "Investigation of Bacteriophage MS2 Viral Dynamics Using Model Discrimination Analysis and the Implications for Phage Therapy." Biotechnology Progress **22**(6): 1650-1658.

Rogers, J. V., C. V. Parkinson, et al. (2008). "A preliminary assessment of silver nanoparticle inhibition of monkeypox virus plaque formation." Nanoscale Research Letters **3**(4): 129-133.

Roselli, M., A. Finamore, et al. (2003). "Zinc Oxide Protects Cultured Enterocytes from the Damage Induced by Escherichia coli." J. Nutr. **133**(12): 4077-4082.

Sambhy, V., M. M. MacBride, et al. (2006). "Silver Bromide Nanoparticle/Polymer Composites: Dual Action Tunable Antimicrobial Materials." Journal of the American Chemical Society **128**(30): 9798-9808.

Sawai, J. (2003). "Quantitative evaluation of antibacterial activities of metallic oxide powders (ZnO, MgO and CaO) by conductimetric assay." Journal of Microbiological Methods **54**(2): 177-182.

Shin, G.-A. and M. D. Sobsey (2003). "Reduction of Norwalk Virus, Poliovirus 1, and Bacteriophage MS2 by Ozone Disinfection of Water." Appl. Environ. Microbiol. **69**(7): 3975-3978.

Shirasaki, N., T. Matsushita, et al. (2009). "Comparison of behaviors of two surrogates for pathogenic waterborne viruses, bacteriophages Q[beta] and MS2, during the aluminum coagulation process." Water Research **43**(3): 605-612.

Silver, S. (2003). "Bacterial silver resistance: molecular biology and uses and misuses of silver compounds." FEMS Microbiology Reviews **27**(2-3): 341-353.

Sobsey, M. D., D. A. Battigelli, et al. (1998). "RT-PCR amplification detects inactivated viruses in water and wastewater." Water Science and Technology **38**(12): 91-94.

Sondi, I. and B. Salopek-Sondi (2004). "Silver nanoparticles as antimicrobial agent: A case study on E. coli as a model for Gram-negative bacteria." Journal of Colloid and Interface Science **275**(1): 177-182.

Sreeja, R., P. M. Aneesh, et al. (2009). "Size-dependent optical nonlinearity of Au nanocrystals." Journal of the Electrochemical Society **156**(10).

Stoimenov, P. K., R. L. Klinger, et al. (2002). "Metal oxide nanoparticles as bactericidal agents." Langmuir **18**(17): 6679-6686.

Tam, K. H., A. B. DjurisÌŒicÌ•, et al. (2008). "Antibacterial activity of ZnO nanorods prepared by a hydrothermal method." Thin Solid Films **516**(18): 6167-6174.

Tang, E., G. Cheng, et al. (2006). "Surface modification of zinc oxide nanoparticle by PMAA and its dispersion in aqueous system." Applied Surface Science **252**(14): 5227-5232.

Thurston-Enriquez, J. A., C. N. Haas, et al. (2003). "Inactivation of Feline Calicivirus and Adenovirus Type 40 by UV Radiation." Appl. Environ. Microbiol. **69**(1): 577-582.

Turkoglu, M. and S. Yener (1997). "Design and in vivo evaluation of ultrafine inorganic-oxide-containing-sunscreen formulations." International Journal of Cosmetic Science **19**(4): 193-201.

Xiong, A. and R. K. Jayaswal (1998). "Molecular Characterization of a Chromosomal Determinant Conferring Resistance to Zinc and Cobalt Ions in Staphylococcus aureus." J. Bacteriol. **180**(16): 4024-4029.

Xiong, M., G. Gu, et al. (2003). "Preparation and characterization of poly(styrene butylacrylate) latex/nano-ZnO nanocomposites." Journal of Applied Polymer Science **90**(7): 1923-1931.

Y. Liu, L. H. A. M. H. L. Z. Q. H. M. L. (2009). "Antibacterial activities of zinc oxide nanoparticles against *Escherichia coli* O157:H7." Journal of Applied Microbiology **9999**(9999).

Yamamoto, O. (2001). "Influence of particle size on the antibacterial activity of zinc oxide." International Journal of Inorganic Materials **3**(7): 643-646.

Yamanaka, M., K. Hara, et al. (2005). "Bactericidal Actions of a Silver Ion Solution on Escherichia coli, Studied by Energy-Filtering Transmission Electron Microscopy and Proteomic Analysis." Appl. Environ. Microbiol. **71**(11): 7589-7593.

Young, R. (1992). "Bacteriophage lysis: mechanism and regulation." Microbiol Rev **56**(3): 430-81.

Young, R., I. N. Wang, et al. (2000). "Phages will out: Strategies of host cell lysis." Trends in Microbiology **8**(3): 120-128.

Zhang, L., Y. Jiang, et al. (2007). "Investigation into the antibacterial behaviour of suspensions of ZnO nanoparticles (ZnO nanofluids)." Journal of Nanoparticle Research **9**(3): 479-489.

Zhang, X., X. He, et al. (2009). "Biosynthesis of size-controlled gold nanoparticles using fungus, Penicillium sp." Journal of Nanoscience and Nanotechnology **9**(10): 5738-5744.

Zodrow, K., L. Brunet, et al. (2009). "Polysulfone ultrafiltration membranes impregnated with silver nanoparticles show improved biofouling resistance and virus removal." Water Research **43**(3): 715-723.